



HAL
open science

A Computable Form for LoRa Performance Estimation: Application to Ricean and Nakagami Fading

Jules Courjault, Baptiste Vrigneau, Olivier Berder, Manav R Bhatnagar

► To cite this version:

Jules Courjault, Baptiste Vrigneau, Olivier Berder, Manav R Bhatnagar. A Computable Form for LoRa Performance Estimation: Application to Ricean and Nakagami Fading. IEEE Access, 2021, 9, pp.81601 - 81611. 10.1109/access.2021.3074704 . hal-03473400

HAL Id: hal-03473400

<https://hal.inria.fr/hal-03473400>

Submitted on 9 Dec 2021

HAL is a multi-disciplinary open access archive for the deposit and dissemination of scientific research documents, whether they are published or not. The documents may come from teaching and research institutions in France or abroad, or from public or private research centers.

L'archive ouverte pluridisciplinaire **HAL**, est destinée au dépôt et à la diffusion de documents scientifiques de niveau recherche, publiés ou non, émanant des établissements d'enseignement et de recherche français ou étrangers, des laboratoires publics ou privés.

Received March 16, 2021, accepted April 4, 2021, date of publication April 21, 2021, date of current version June 11, 2021.

Digital Object Identifier 10.1109/ACCESS.2021.3074704

A Computable Form for LoRa Performance Estimation: Application to Ricean and Nakagami Fading

JULES COURJAULT¹, BAPTISTE VRIGNEAU¹, OLIVIER BERDER¹, (Member, IEEE),
AND MANAV R. BHATNAGAR², (Senior Member, IEEE)

¹Univ Rennes, CNRS, IRISA, 22300 Lannion, France

²Department of Electrical Engineering, Indian Institute of Technology Delhi, New Delhi 110016, India

Corresponding author: Olivier Berder (olivier.berder@irisa.fr)


ABSTRACT Emerging applications such as connected farms, wildness monitoring, smart cities, and Factory of the Future leverage emerging Low Power Wide Area Networks (LPWAN), allowing a good trade-off between radio range, data rate, and energy consumption. However, only few theoretical studies of these recent technologies are available to help network designers to optimize real field deployments or even achieve real-time adaptation of transmission parameters. A new approach based on Marcum function is proposed in this paper to estimate – in a fast and accurate manner – the performance in terms of Bit Error Rate of LoRa, one of the most used LPWAN technologies. The method is proposed for Gaussian channels, over challenging propagation environments, i.e., Ricean and Nakagami fading. Simulation results show that our proposed approximation reduces the approximation error about one order of magnitude compared to existing ones and can be computed by classical software.

INDEX TERMS Accurate approximation, fading channels, Internet of Things, LoRa performance, low-power wide area networks, Marcum function.

I. INTRODUCTION

In the last decade, the number of connected devices has increased exponentially, giving birth to the Internet of Things (IoT) [1] and its applications such as connected farms [2]–[5], wildness monitoring, smart cities or Factory of the Future. Most of these applications require transmission of data over long distances at a reasonable energy cost. Emerging standards known as Low Power Wide Area Networks (LP-WAN) respect these requirements by proposing trade-offs between transmission range, data rate, and energy consumption [6]–[8].

Among all available candidates, LoRa (Long Range) technology [9], [10], has already become popular in many countries. LoRa communications can use ISM frequency bands at 433 MHz, 868 MHz, or 915 MHz, with a data rate that can reach up to 50 kbps. LoRa leverages Chirp Spread Spectrum (CSS) modulation with a linear variation of frequency over the time [11], [12], which allows reduction of both

The associate editor coordinating the review of this manuscript and approving it for publication was Md. Arafatur Rahman .

interference and Doppler effects. This modulation can be configured with three parameters: the bandwidth BW , the spreading factor SF , and the code rate CR .

A main challenge of IoT is to deal with a huge number of nodes. The behavior of such a network, e.g. the network congestion, the achieved quality of service, or the impact of duty cycle of nodes on medium occupancy, is generally studied through simulators [13], [14]. Some studies focus on the scalability [15] of IoT networks or the energy consumption of IoT nodes [16], [17]. A mathematical tool for tuning the LoRa parameters could therefore be very convenient for efficient network design.

Although the LoRa technology is well explained in the patent [9], rigorous theoretical studies of this technology are still missing. In [18], a mathematical approach allowed to rigorously study the modulation and demodulation processes of LoRa, but it lacks a theoretical analysis of the Bit Error Rate (BER). Previously in [19] and more recently in [20], exact expressions of the BER of LoRa over several channels models were presented, including Nakagami- m and Ricean fading channels. As explained in [19], [21], computational

issues remain with classical software (e.g. Matlab, Octave, and Python) due to high values of binomial coefficients that potentially lead to aberrant results.

To avoid this, authors of [12], [22] provided some LoRa BER approximations based on Monte-Carlo simulations and curve fitting for Gaussian channels. Further, the authors in [23] combined theoretical results and Monte Carlo simulations for performance analysis of LoRa over Gaussian channels. On the other hand, there exist very few works considering the effect of fading channels on the performance of LoRa, and only the authors in [21] proposed an analytical BER computation approach for the analytical error performance of LoRa over both additive Gaussian and Rayleigh fading channels. A new approach to approximate the BER of a LoRa transmission has been recently proposed in [24] and [25], respectively, for additive Gaussian and Rayleigh fading channels, and the analytical results are based on the Marcum function [26], well known in communication theory.

The main contributions of this work are:

- A thorough description of the approximation methodology leveraging Marcum function to express the Gaussian noise impact.
- Accurate BER approximations for common fading channel models, namely Nakagami and Ricean (both including Rayleigh fading as a special case).
- Asymptotic BER expressions at high Signal-to-Noise Ratio (SNR) giving insights into diversity order and coding gain.
- Validations of the accuracy of the proposed expressions through exhaustive simulations.
- A study of the impact of K and m fading parameters on the SNR loss for a given target BER with respect to the Additive White Gaussian Noise (AWGN) case.

The rest of the paper is organized as follows. Section II summarizes the State of the Art (SoA) on LoRa performance estimation and justifies the need for approximations. The essence of this new approach based on Marcum function is presented in Section III with first results on Gaussian and Rayleigh channels. This idea is next generalized to various channel fading in Section IV, while simulation results highlighting the accuracy of the proposed approximations are shown in Section V. Lastly, Section VI draws the conclusions and future works.

II. RELATED WORKS ON LoRa PERFORMANCE

This section first introduces the demodulation principle and then the theoretical BER expression of the CSS performance in an AWGN environment, and the computation problem induced. Due to this issue, several existing works on approximation of the theoretical BER of LoRa will be presented in a second paragraph.

A. LoRa MODULATOR AND DEMODULATOR

In LoRa, SF is defined as the logarithm in base 2 of the number of chirps per symbol. LoRa operates with SF

from 7 to 12. LoRa uses three bandwidths: 125 kHz, 250 kHz and 500 kHz. A LoRa symbol is therefore composed of $N = 2^{SF}$ chirps covering the entire bandwidth, starting with a series of upward (or downward) chirps from an initial frequency, which represents a symbol. The frequency wraps around to the minimum frequency (or maximum frequency with down-chirp) when the maximum (minimum with down-chirp) of the bandwidth is reached. A linear chirp signal is usually defined by:

$$s(t) \triangleq A \times e^{j\left(2\pi\left(f_0t + \frac{\mu t^2}{2}\right) + \phi_0\right)}, \quad (1)$$

where ϕ_0 is the initial phase, A the amplitude, μ the chirp rate, $f_0 = lBW/2^{SF}$ is the starting frequency of chirp corresponding to the symbol l , and $\phi(t) = 2\pi\left(f_0t + \frac{\mu t^2}{2}\right) + \phi_0$ is the instantaneous phase at time t . From (1) the corresponding instantaneous frequency is given by:

$$f(t) = \frac{d\phi(t)}{2\pi dt} = f_0 + \mu t. \quad (2)$$

Applying CSS to LoRa modulation, each frequency f_0 in the band represents a symbol. When reaching the maximum value of the bandwidth, the instantaneous frequency falls back to the minimum value of the bandwidth, and is therefore expressed as follows:

$$f(t) = f_{\min} + [(\Delta f_0 + \mu t) \bmod BW], \quad (3)$$

where $\Delta f_0 = f_0 - f_{\min}$ and f_{\min} is the minimum frequency of the bandwidth.

With N chirps, a code word can contain SF information bits. The duration T_s of a symbol is given by $T_s = 2^{SF}/BW$. For a given bandwidth, increasing the spreading factor by one unit doubles the Time-on-Air (ToA) to transmit the same amount of data, resulting in a decreased bit rate. The bit rate is calculated by:

$$R_b = SF \times \frac{BW}{2^{SF}}. \quad (4)$$

The third parameter in the configuration of LoRa modulation is the code rate. LoRa can use Forward Error Correction (FEC) code for each block of four information bits. The number of redundant bits for each block varies from one to four, corresponding to CRs of 4/5, 4/6, 4/7 and 4/8. Then, the bit stream is processed by an interleaver to make FEC code more robust to burst errors. Additionally, a whitening structure can also be used to make the signal like white noise, thus avoiding frequency selective channel penalties.

Fig. 1 illustrates the main steps of the non-coherent demodulator:

- 1) Sampling the signal with the period $T_e = 1/BW$.
- 2) Multiplying with a down chirp defined by $c(t) \triangleq e^{-j2\pi\mu t^2/2}$
- 3) Performing the Fast Fourier Transform (FFT). The theoretical study in [18] showed that the FFT result is a Dirac impulse centered on the starting frequency. Thus, finding this frequency leads to the symbol value.

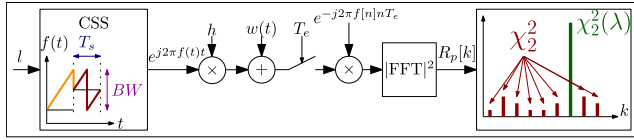


FIGURE 1. Principle of LoRa demodulator with the main steps: sampling, down chirping, FFT, and maximum rule decision.

- 4) Applying the maximum value criterion on the squared modulus is the classical solution to estimate the desired frequency.

When an independent and identically distributed (i.i.d.) AWGN is considered, the noise after the FFT is also i.i.d. AWGN, thus the wrong-detected symbol can be among the $N - 1$ remaining symbols with the same probability. Consequently, since the symbol error probability is the same for each transmit symbol, the study can focus on only ones case.

B. LoRa BER THEORETICAL EXPRESSION AND ISSUES

Let l denote the transmit symbol index, and let $\bar{\mathbb{P}}_l$ denote the conditional probability of a right detection knowing the noise realization. According to [19, p.217], [21], this probability can be expressed as follows:

$$\bar{\mathbb{P}}_l = F_{\chi^2} \left(\frac{|\sqrt{N} + W_p[N - l]|^2}{\sigma_n^2} \right)^{N-1}, \quad (5)$$

where $N = 2^{SF}$ is the number of chirps, and $W_p[N - l]$ is a zero mean complex Gaussian noise of variance σ_n^2 . By using the cumulative density function (cdf) of a χ^2 random variable with 2 degrees of freedom, i.e., $F_{\chi^2}(x) = 1 - \exp(-\frac{x}{\sigma_n^2})$, (5) can be written:

$$\bar{\mathbb{P}}_l = \left(1 - \exp \left(-\frac{|\sqrt{N} + W_p[N - l]|^2}{\sigma_n^2} \right) \right)^{N-1}. \quad (6)$$

Let us define a new random variable:

$$Z \triangleq 2\gamma|\sqrt{N} + W_p[N - l]|^2, \quad (7)$$

where $\gamma = 1/\sigma_n^2$ is the average SNR. It can be observed from (7) that Z follows a non-central χ^2 distribution with 2 degrees of freedom and the noncentrality parameter $\lambda = 2N\gamma$. Its probability density function (pdf) is expressed as:

$$f_Z(x) = \frac{1}{2} \exp \left(-\frac{x + \lambda}{2} \right) I_0(\sqrt{\lambda x}), \quad (8)$$

where $I_0(\cdot)$ is the modified Bessel function of the second kind of order 0. Lastly, the average Symbol Error Rate (SER) is obtained as follows:

$$\text{SER}(\gamma) = \int_0^{+\infty} \left(1 - \left(1 - e^{-z/2} \right)^{N-1} \right) f_Z(z) dz \quad (9)$$

$$= \frac{1}{N} \sum_{k=1}^{N-1} C_N^{k+1} (-1)^{k+1} \int_0^{+\infty} e^{-\frac{kz}{2}} f_Z(z) dz \quad (10)$$

$$= \frac{1}{N} \sum_{k=1}^{N-1} C_N^{k+1} (-1)^{k+1} e^{-N\gamma \frac{k}{(k+1)}}, \quad (11)$$

where (9) is obtained by marginalization of (6) over the pdf of (8), (10) is derived by using polynomial expansion of $(1 - e^{-z/2})^{N-1}$ in (9), and (11) is found by using the characteristic function of a non-central χ^2 distribution in (10). Further, in (10) and (11), $C_N^{k+1} = N!/((k + 1)!(N - k - 1)!)$ is the binomial coefficient.

C. EXISTING APPROXIMATIONS OF THE BER

A relation between BER and SER of LoRa is given by [19, p.218]:

$$\text{BER}(\gamma) = \frac{2^{SF-1}}{2^{SF} - 1} \text{SER}(\gamma). \quad (12)$$

An approximate BER of LoRa over Gaussian channel is given as [22, Eq.(3)]:

$$\text{BER}(\gamma) \approx Q \left(\frac{\log_{12}(SF)}{\sqrt{2}} \gamma \right), \quad (13)$$

where $Q(x)$ the Gaussian q-function or the tail distribution of the standard normal distribution. Another study in [12] provided the following approximate expression of the BER of LoRa over Gaussian channel that relies on numerical fitting [12, Eq.(21)]:

$$\text{BER}(\gamma) \approx 0.5 \cdot Q \left(1.28\sqrt{SF \cdot \gamma} - 1.28\sqrt{SF} + 0.4 \right). \quad (14)$$

Recently, the authors in [21] proposed two new accurate estimations of the BER for LoRa communications in AWGN and Rayleigh fading channels. The principle is to approximate a Ricean distribution by a Gaussian one, and the approximate BER expression for AWGN channel is [21, Eq.(21)]:

$$\text{BER}(\gamma) \approx 0.5 \cdot Q \left(\frac{\sqrt{N \cdot \gamma} - \left(H_{N-1}^2 - \frac{\pi^2}{12} \right)^{1/4}}{\sqrt{H_{N-1} - \sqrt{H_{N-1}^2 - \frac{\pi^2}{12} + 0.5}}} \right), \quad (15)$$

where H_k is the k^{th} harmonic number which can be approximated by $\log(k) + \frac{1}{2k} + 0.57722$. Another approximation is obtained from the former with some simplifications and approximations [21, Eq.(23)]:

$$\text{BER}(\gamma) \approx 0.5 \cdot Q \left(\sqrt{2N \cdot \gamma} - \sqrt{1.386 \cdot SF + 1.154} \right). \quad (16)$$

In [21], the authors also extended the result to the Rayleigh fading [21, Eq.(33)]:

$$\text{BER} \approx 0.5 \cdot \left(Q \left(-\sqrt{2H_{N-1}} \right) - \sqrt{\frac{N\gamma}{N\gamma+1}} e^{\frac{H_{N-1}}{N\gamma+1}} Q \left(-\sqrt{2H_{N-1} \frac{N\gamma}{N\gamma+1}} \right) \right). \quad (17)$$

III. MARCUM-FUNCTION BASED APPROXIMATION FOR AWGN CHANNEL

In order to find a computable approximation of the SER for various fading channels, the first step is to deal with AWGN channel, approximating $\bar{\mathbb{P}}_l$ instead of the pdf of the random variable Z involved in the SER derivation.

A. APPROXIMATION OF $\bar{\mathbb{P}}_j$

As discussed above, the previous works focused on approximating Chi-squared or Ricean distributions with a Gaussian one. The novelty of the present work is to find an approximation of $g(z) = 1 - (1 - e^{-z/2})^{N-1}$ while keeping the non-central Chi-squared distribution unaltered. When $g(z)$ is expanded as a sum, the term $e^{-kz/2}$ is less significant for large values of k and z . Thus, the sum can be limited to ϵ terms. It is equivalent to find the approximation based on the Taylor's series of order ϵ for high values of z . Consequently, the first main approximation is:

$$g(z) \approx \tilde{g}(z) = \sum_{k=1}^{\epsilon} (-1)^{k+1} C_{N-1}^k e^{-kz/2}. \quad (18)$$

Fig. 2 shows the comparison with the exact values of $g(z)$ and different approximation orders, $\epsilon = 1$ to 7. The good point is that binomial coefficients are limited to low values of k , which solves one of the computational issue. Since N is high, especially for $SF = 12$, the binomial coefficient C_{N-1}^k will suffer from loss of precision, typically when k is superior to 5 for $SF = 12$ when using Matlab. The drawback is that, although the approximation is tight for large values of z , the divergence is problematic: as z goes to zero, the approximation tends toward infinity for odd values of ϵ and toward zero for even orders. Nevertheless, a simple and efficient approximation based on a piecewise definition is given by:

$$g(z) \simeq \begin{cases} 1 & \text{if } z \leq z_c \\ \tilde{g}(z) & \text{if } z > z_c, \end{cases} \quad (19)$$

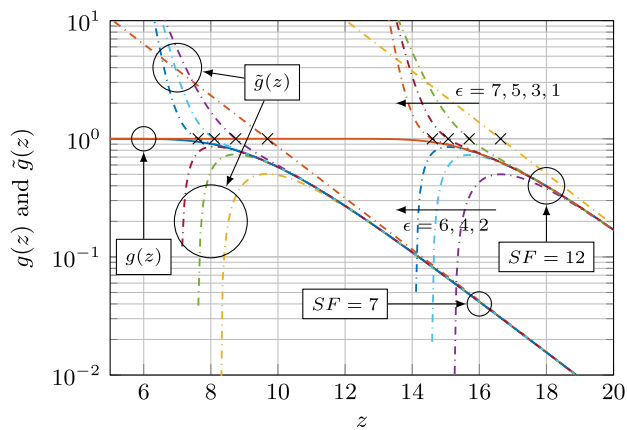


FIGURE 2. Comparison of the exact function $g(z)$ and approximations with different orders, i.e., ϵ varying from 1 to 7 and $SF = 7, 12$. Values of z_c are plotted with cross marker.

where z_c is a threshold depending on the values of ϵ and SF that will be discussed in the next paragraph. The different values of z_c are available in Fig. 2 and a first quick observation is that the piecewise approximation should be accurate for low values of ϵ . The next step is to compute the expectation

of $g(z)$ by using the approximation (19), leading to the following result (proof in appendix A):

$$\text{SER}(\gamma) = 1 + \frac{1}{N} \sum_{k=1}^{\epsilon+1} C_N^k (-1)^k \times e^{-\frac{N \cdot \gamma (k-1)}{k}} Q_1 \left(\sqrt{\frac{2N}{k}} \gamma, \sqrt{kz_c} \right), \quad (20)$$

where $Q_1(\cdot, \cdot)$ denotes the Marcum function of order 1 defined by:

$$Q_1(a, b) \triangleq \int_b^{\infty} x e^{-\frac{x^2+a^2}{2}} I_0(ax) dx. \quad (21)$$

B. HOW TO FIND THE THRESHOLD z_c

All parameters are known for computing (20) except the value of z_c . The problem is not trivial and let us propose a solution for low values of the order ϵ . Note that the results in the next section and the above remark confirm that the order does not need to be greater than 7. First, by applying the variable change $X = e^{-\frac{z}{2}}$ in (18), solving $\tilde{g}(z) = 1$ is equivalent to find the roots of a ϵ -order polynomial. Since the approximation with even values of ϵ cannot reach the unity value, as shown in Fig. 2, the study is limited to odd value cases. The only known assumption is that z_c is the unique positive real root. However, we are able to obtain the exact solutions for $\epsilon = 1$, by solving the first order polynomial, and for $\epsilon = 3$, by using a symbolic computation software. By using the notation $z_c(\epsilon)$, those exact solutions are expressed as:

$$z_c(1) = 2 \log(N - 1), \quad (22)$$

and

$$z_c(3) = -2 \log \left(\tau - \frac{N - 4}{(N - 2)(N - 3)^2} \frac{1}{\tau} + \frac{1}{N - 3} \right). \quad (23)$$

where $\tau = \left(\frac{(N-4)(N-5)}{(N-1)(N-2)(N-3)^3} + \frac{\sqrt{2}(N-4)}{(N-1)(N-2)^{1.5}(N-3)^{1.5}} \right)^{\frac{1}{3}}$, $z_c(\epsilon) = -2 \log(X_c(\epsilon))$ and $X_c(\epsilon)$ is the unique real solution of

$$\sum_{k=1}^{\epsilon} (-1)^{k+1} C_{N-1}^k X^k = 1. \quad (24)$$

As two exact roots are available, we propose a polynomial function of order 1 that gives the exact values of z_c for $\epsilon = 1, 3$ and an approximation for higher values:

$$z_c(\epsilon) = -2 \log(\alpha_1 \epsilon + \alpha_0), \quad (25)$$

$$\alpha_0 = (3e^{-z_c(1)/2} - e^{-z_c(3)/2})/2, \quad (26)$$

$$\alpha_1 = (e^{-z_c(3)/2} - e^{-z_c(1)/2})/2. \quad (27)$$

Fig. 3 shows the comparison between a numerical solving of z_c and the proposed approximation. We can observe from the figure that the approximation is still tight to the numerical value for $\epsilon = 5, 7$. Note that the proposed approximation is not suitable for higher values of ϵ . Concerning the even

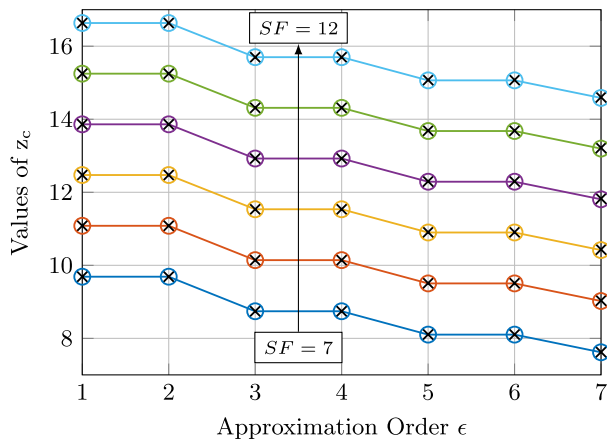


FIGURE 3. Approximation of the threshold z_c : numerical solutions are plotted with crosses and the approximation with circles.

cases, we propose to define z_c as the value maximizing $\tilde{g}(z)$, i.e., z_c is the solution to the equation $\frac{\partial \tilde{g}(z)}{\partial z} = 0$, leading also to a polynomial root. However, polynomial coefficients are similar but different, and the same study for odd cases can be applied. A numerical solving of $\frac{\partial \tilde{g}(z)}{\partial z} = 0$ and a graphical comparison from Fig. 2 shows that result for even and odd cases are very close. For example, the cases $\epsilon = 1$ and $\epsilon = 2$ lead to $N - 1$ and $N - 2$, respectively. For conciseness, we propose a heuristic approximation $z_c(\epsilon) = z_c(\epsilon - 1)$ when ϵ is even, as shown in Fig. 3. When N is larger than 1, which holds for all LoRa SF, the following simplifications are available:

$$z_c(1) \simeq 2 \log(N) = 2 \log(2)SF, \quad (28)$$

$$z_c(3) \simeq 2 \log\left(\frac{N}{a}\right) = z_c(1) - 2 \log(a), \quad (29)$$

$$z_c(\epsilon) \simeq z_c(1) - 2 \log\left(\left(\frac{3-a}{2} + \frac{(a-1)}{2}\epsilon\right)\right), \quad (30)$$

with $a = (1 + \sqrt{2})^{1/3} - 1/(1 + \sqrt{2})^{1/3} + 1$.

IV. SER COMPUTATION OVER FADING CHANNELS

The second challenge of our work is to take into consideration the effect of the channel. To this aim, we extend the previous result for AWGN to Ricean, Nakagami, and Rayleigh fading channels. The proposed results represent fast and accurate approximations, computable with classical programming languages, such as Matlab, Python, or C.

A. PROBLEM STATEMENT

Let us assume now a fading gain associated with an AWGN. The received signal is expressed as:

$$r(t) = hs(t) + w(t), \quad (31)$$

where h denotes the channel fading coefficient, $s(t)$ is the LoRa chirp, and $w(t)$ is an additive Gaussian noise. The term h is an iid complex random variable and it is assumed that the fading channel is block fading during the LoRa transmission,

i.e., h is constant for a full LoRa symbol and will change for the next one. After the demodulation, by using the linearity property of the Fourier transform, the obtained signal is:

$$R_p[k] = h\sqrt{N}\delta(k + l - N) + W_p[k]. \quad (32)$$

Thus, the probability $\bar{\mathbb{P}}_l$ given the value h that the right symbol is decoded is expressed as:

$$\begin{aligned} \bar{\mathbb{P}}_l &= \Pr\left[\forall k \neq N-1 : |R_p[k]|^2 < |R_p[N-l]|^2\right] \\ &= \prod_{\substack{k=0 \\ k \neq N-l}}^{N-1} \Pr\left[|W_p[k]|^2 < |h\sqrt{N} + W_p[N-l]|^2\right] \\ &= F_{\chi^2_2}\left(\frac{|h\sqrt{N} + W_p[N-l]|^2}{\sigma_n^2}\right)^{N-1}. \end{aligned} \quad (33)$$

As described above for the Gaussian case, we obtain

$$\bar{\mathbb{P}}_l = \left(1 - \exp\left(-\frac{|h\sqrt{N} + W_p[N-l]|^2}{\sigma_n^2}\right)\right)^{N-1}. \quad (34)$$

Let us denote the variable Z as:

$$Z \triangleq \gamma \cdot |h\sqrt{N} + W_p[N-l]|^2. \quad (35)$$

The random variable Z follows a non-central chi-squared distribution with 2 degrees of freedom with the non-central parameter $\lambda = \gamma \cdot 2|h|^2 N$. The link between SER with a fading gain and AWGN case from (20) is then $\text{SER}(|h|^2\gamma)$. In order to obtain the SER, the distribution of h must be defined and the average computed as follows;

$$\text{SER}_h(\gamma) = \int_0^{+\infty} \text{SER}(x\gamma)f_{|h|^2}(x)dx, \quad (36)$$

where $f_{|h|^2}(x)$ is the pdf of the squared modulus of h . The previous result based on Marcum function will be used and the difficulty is to deal with it in the integral:

$$\begin{aligned} \text{SER}_h(\gamma) &= 1 + \frac{1}{N} \sum_{k=1}^{\epsilon+1} C_N^k (-1)^k \\ &\times \int_0^{+\infty} e^{-\frac{N\gamma x(k-1)}{k}} Q_1\left(\sqrt{\frac{2N}{k}}\gamma x, \sqrt{kz_c}\right) \\ &\times f_{|h|^2}(x)dx. \end{aligned} \quad (37)$$

B. APPLICATION TO DIFFERENT FADING MODELS

Most fading channels can be modeled by Nakagami and Ricean distributions (Rayleigh distribution is a special case of both). This section aims at presenting SER approximations for these channels, using the method described in previous section. Only theorems are presented hereafter, all mathematical derivations can be found in appendix B.

Theorem 1: • The SER for Nakagami fading with the real $m \geq 1/2$, is approximated by (38), as shown at the bottom of the next page, where $\bar{\gamma} = N\gamma/m$, ${}_1F_1(a; b; x)$ is the confluent hypergeometric function, and $\Phi_2(a, b; c; x, y)$ is the second Humbert function.

- The SER for a Ricean fading with the positive real K is approximated by (39), as shown at the bottom of the page, where $\bar{\gamma} = N\gamma/(1 + K)$.
 - The SER for a Rayleigh fading is approximated by (40), as shown at the bottom of the page, where $\bar{\gamma} = N\gamma$.
- Proof:* see Appendix B ■

In order to reduce the complexity of the computation we propose an asymptotic approximation for high values of SNR from results in Theorem 1. This approach also gives a direct insight into diversity order, as will be shown in Section V.

Theorem 2: • The SER under a Nakagami fading with the parameter m is approximated at high SNR by:

$$SER_{Naka}(\bar{\gamma}) \simeq \frac{\mathcal{A}_{Naka}}{\bar{\gamma}^m}, \quad (41)$$

where $\bar{\gamma} = N\gamma/m$ and \mathcal{A}_{Naka} is defined in (42), as shown at the bottom of the next page.

- The SER under a Ricean fading with the parameter K is approximated at high SNR by:

$$SER_{Rice}(\bar{\gamma}) \simeq \frac{\mathcal{A}_{Rice}}{\bar{\gamma}}, \quad (43)$$

where $\bar{\gamma} = N\gamma/(1 + K)$ and \mathcal{A}_{Rice} is defined as:

$$\mathcal{A}_{Rice} = e^{-K} \left(\frac{z_c}{2} + \sum_{k=2}^{\epsilon+1} (-1)^k \frac{C_N^k}{N} \frac{k}{k-1} e^{-\frac{z_c}{2}(k-1)} \right). \quad (44)$$

- The SER under a Rayleigh fading is approximated at high SNR by:

$$SER_{Ray}(\bar{\gamma}) \simeq \frac{1}{\bar{\gamma}} \mathcal{A}_{Ray}, \quad (45)$$

where $\bar{\gamma} = N\gamma$ and \mathcal{A}_{Ray} is defined as

$$\mathcal{A}_{Ray} = \left(\frac{z_c}{2} + \sum_{k=2}^{\epsilon+1} (-1)^k \frac{C_N^k}{N} \frac{k}{k-1} e^{-\frac{z_c}{2}(k-1)} \right). \quad (46)$$

Proof: see Appendix C ■

One should note that those expressions are easy to compute and the binomial coefficient is not an issue thanks to the low values of ϵ (between 1 and 7). It will be shown in Section V that those approximations are accurate at high SNR whatever the LoRa configuration and channel parameters.

V. NUMERICAL RESULTS

This section presents the results obtained with the proposed approximations, all tested with both Matlab/Octave and Python functions. The first subsection compares our solution with the state of the art for available channels, i.e., AWGN and Rayleigh fading to highlight the accuracy gain. The second subsection validates the Nakagami and Ricean cases thanks to simulations, and the high-SNR approximation is also plotted. Finally we study the impact of fading channel parameters m and K on the BER.

A. BER OVER AWGN AND RAYLEIGH FADING

Fig. 4 compares the proposed approximation (20) with the best of the SoA [21, Eqs. (21) and (23)] and the theoretical expression of the BER in AWGN channel (9), computed numerically by using trapezoidal method on the integral. Even though this method can be used in the case of AWGN channel, it is not recommended for fading channels. Indeed, for fading channels we need to compute two improper integrals, which make the computation far more complex and less accurate. As we can see, the proposed approximation is valid, and is more accurate than [21, Eq. (23)].

To get a better idea of the gain on the accuracy, Fig. 5 compares the approximation to theoretical BER ratio, defined by $R = \frac{SER_{approx}}{SER_{theo}}$, where SER_{approx} is the considered approximation for AWGN channel, and SER_{theo} is the theoretical BER, computed by using (9) by numerically computing the integral. It can be observed from the figure that the accuracy of the proposed approximation is better than the existing ones for all SNR values considered in the figure. It can be seen from Fig. 5 that for existing approximations a divergence occurs,

$$SER_{Naka}(\bar{\gamma}) = 1 + \sum_{k=1}^{\epsilon+1} \frac{C_N^k}{N} (-1)^k \times \left(\left(\bar{\gamma} \frac{k-1}{k} + 1 \right)^{-m} + (\bar{\gamma} + 1)^{-m} e^{-\frac{z_c k}{2}} \left({}_1F_1 \left(m; 2; \frac{z_c}{2} \frac{\bar{\gamma}}{\bar{\gamma} + 1} \right) - \Phi_2 \left(1, m; 1; \frac{z_c k}{2}, \frac{z_c}{2} \frac{\bar{\gamma}}{\bar{\gamma} + 1} \right) \right) \right) \quad (38)$$

$$SER_{Rice}(\bar{\gamma}) = 1 + \sum_{k=1}^{\epsilon+1} \frac{C_N^k}{N} (-1)^k \left(\bar{\gamma} \frac{k-1}{k} + 1 \right)^{-1} e^{-K \frac{\bar{\gamma} k-1}{\bar{\gamma} \frac{k-1}{k} + 1}} Q_1 \left(\sqrt{\frac{2K}{k} \frac{\bar{\gamma}}{(\bar{\gamma} \frac{k-1}{k} + 1)(\bar{\gamma} + 1)}}, \sqrt{k z_c \frac{\bar{\gamma} \frac{k-1}{k} + 1}{\bar{\gamma} + 1}} \right) \quad (39)$$

$$SER_{Ray}(\bar{\gamma}) = 1 + \sum_{k=1}^{\epsilon+1} \frac{C_N^k}{N} (-1)^k \left(\bar{\gamma} \frac{k-1}{k} + 1 \right)^{-1} e^{-\frac{k z_c (\bar{\gamma}(k-1)/k + 1)}{2(\bar{\gamma} + 1)}} \quad (40)$$

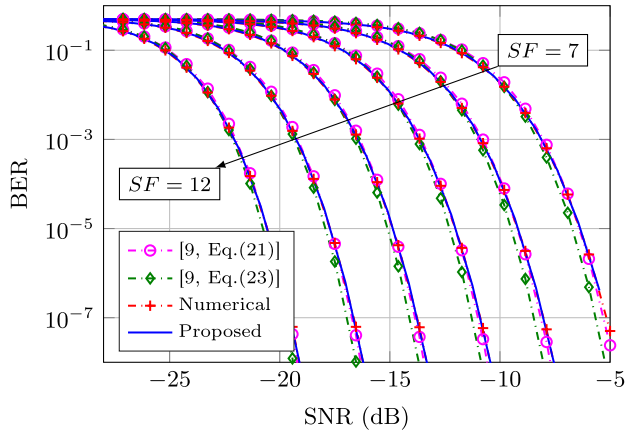


FIGURE 4. Comparison of (20) with [21, Eq. (21)], [21, Eq. (23)] and the theoretical expression, computed numerically by using trapezoidal method on the integral of (9) for $SF \in \{7, 12\}$, over AWGN channel.

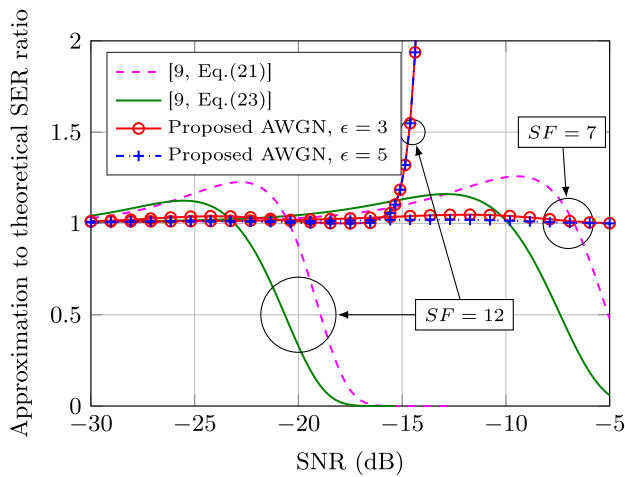


FIGURE 5. Comparison of the approximation to theoretical SER ratio of the proposed approximation for AWGN channel with the best of the SoA. The theoretical SER was computed by using trapezoidal method on the integral of (9).

for lower SNR when SF increases, but the robustness of the proposed approximation is better than SoA. For example, with $SF = 12$, the gain is about 5 dB.

Fig. 6 compares the proposed approximation for a Rayleigh fading channel with [21, Eq. (33)], Monte-Carlo simulations and the high-SNR approximations for $SF \in \{7, 12\}$. The proposed approximation is validated by simulations in the figure. Moreover, it can be seen from the figure that the high-SNR case with $\epsilon = 1$ provides a good approximation with a very simple expression. For this case, the approximation has the same diversity order, i.e., the high SNR expression in (45) shows a diversity of 1.

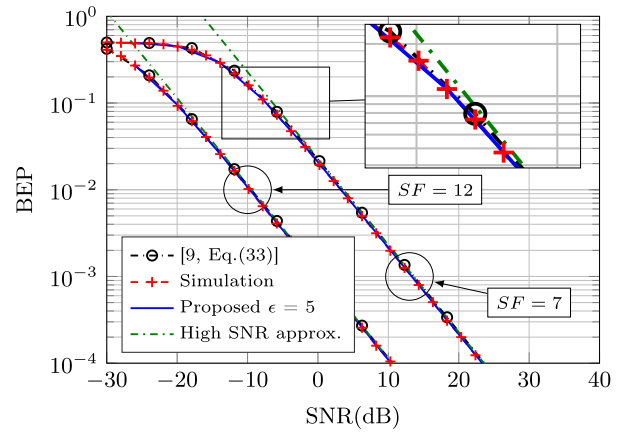


FIGURE 6. Comparison of (40) with [21, Eq.(33)] and Monte-Carlo simulations for $SF \in \{7, 12\}$, over Rayleigh fading channel.

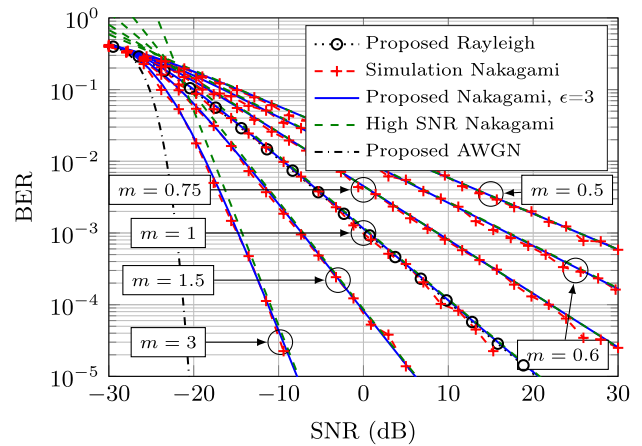


FIGURE 7. Comparison of (38) with Monte-Carlo simulations for $SF = 12$, over Nakagami fading channel with $m \in \{0.5, 0.6, 0.75, 1, 1.5, 3\}$.

B. BER OVER NAKAGAMI AND RICEAN FADINGS

The proposed expression (38) is given for an arbitrary real value of m and the main computation difficulties are about the confluent hypergeometric function and the second Humbert function. However, most of classical software languages provide libraries that include those functions. Moreover, the authors in [27] offered a computation solution to this problem. Fig. 7 shows the BER of LoRa by using the proposed approximation and simulations for different values of m (0.5, 0.6, 0.75, 1, 1.5, 3). It can be seen from the figure that the simulations fit well with the derived expression for Nakagami fading channel. Further, it can be seen from the figure that the proposed high SNR approximation accurately indicates a diversity order of m . Fig. 8 compares the

$$\mathcal{A}_{Naka} = \sum_{k=2}^{\epsilon+1} \frac{C_N^k}{N} (-1)^k \left(\frac{k}{k-1}\right)^m + {}_1F_1\left(m; 2; \frac{z_c}{2}\right) \sum_{k=1}^{\epsilon+1} \frac{C_N^k}{N} (-1)^k e^{-\frac{z_c}{2}k} - \sum_{k=1}^{\epsilon+1} \frac{C_N^k}{N} (-1)^k e^{-\frac{z_c}{2}k} \Phi_2\left(1, m; 1; \frac{z_c k}{2}, \frac{z_c}{2}\right) \quad (42)$$

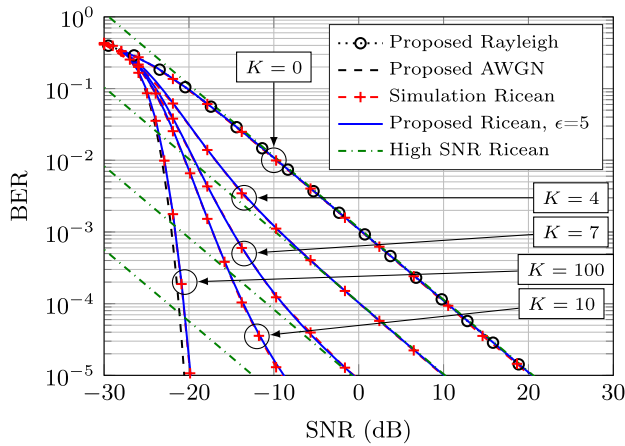


FIGURE 8. Comparison of (39) with Monte-Carlo simulations for $SF = 12$, over Ricean fading channel with $K \in \{0, 4, 7, 10, 100\}$.

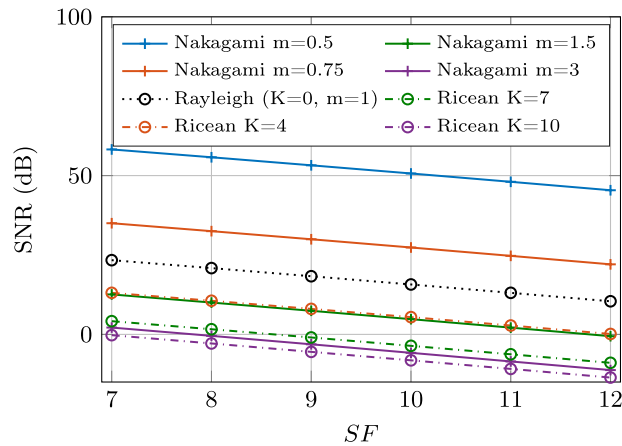


FIGURE 9. Minimum required SNR in dB for a targeted BER of 10^{-4} , under various Ricean or Nakagami fading channels.

proposed approximation (39) and the high SNR approximation (43) with Monte-Carlo simulations for different values of $K(0, 4, 7, 10, 100)$ for $SF = 12$. As it can be seen on the figure, (39) fits well with the Monte-Carlo simulations. Note that for $K = 0$, Rayleigh fading is observed and for $K \rightarrow \infty$, it results into AWGN channel. Consequently, the AWGN and Rayleigh cases are lower and upper bounds, respectively, and the BER has therefore two behaviors: an AWGN-like at low SNR and a Rayleigh one at high SNR. It explains why the high SNR approximation gives a diversity order equal to 1 and the low accuracy of the high SNR approximation (43) when K increases.

C. USECASE: REQUIRED SNR FOR A GIVEN QUALITY OF SERVICE

The quality of service and SNR are linked and the idea of this usecase is to obtain the required SNR for a targeted quality of service over various fading channels. Fig. 9 presents the needed SNR in dB to achieve a BER of 10^{-4} in a Nakagami or

a Ricean fading channel. The SNR was found with a straightforward numerical search by using (38) and (39) with $\epsilon = 3$. As we can see on this figure, independently of the channel configuration, increasing the SF enhances the performance, i.e the required SNR is decreasing. The curves also highlight the impact of the channel parameters K and m .

VI. CONCLUSION

While LoRa standard is now well known and defined in the patent, theoretical studies about performance are not so simple when real propagation environment is considered. Some works are available in the literature but the results are not tractable and cannot be computed with software such as Matlab, Octave or Python. In this paper, we have introduced a new approximation based on Marcum function for an AWGN channel, and we have derived Bit Error Probabilities of LoRa for various fading channels, namely Rayleigh, Ricean or Nakagami. The obtained expressions have been validated by simulations, and comparisons with existing solutions have proved that the proposed solution is more accurate, while being computable on Matlab, Octave and Python. These expressions are very useful to obtain performance estimation of LoRa communications, e.g. varying the spreading factor, over different fading channels. This fast and accurate performance estimation could be associated with network simulators to help network designers before deployment. We have therefore proposed a usecase corresponding to the required SNR for a desired QoS as a function of key-parameters of the channel fading. A next step of this work could be the derivation of the performance in terms of BER for non-Gaussian noises such as α -stable, generalized Gaussian or Middleton noises and then include fading channels.

**APPENDIX A
PROOF OF THE Marcum-Q FUNCTION BASED APPROXIMATION FOR AWGN CHANNEL (18)**

To find the result (20), we need to compute the expectation of the approximation of $g(z)$ (19) as follows:

$$\begin{aligned}
 SER(\gamma) &= \int_0^{z_c} f_Z(z) dz \\
 &+ \int_{z_c}^{+\infty} \left(1 - \sum_{k=0}^{\epsilon} C_{N-1}^k (-1)^k e^{-kz/2} \right) f_Z(z) dz \\
 &= 1 + \sum_{k=1}^{\epsilon+1} C_{N-1}^{k-1} (-1)^k \\
 &\quad \times \int_{z_c}^{+\infty} e^{-\frac{(k-1)z}{2}} \frac{1}{2} e^{-\frac{z+\lambda}{2}} I_0(\sqrt{\lambda z}) dz \\
 &= 1 + \sum_{k=1}^{\epsilon+1} C_{N-1}^{k-1} \frac{(-1)^k}{2} \int_{z_c}^{+\infty} e^{-\frac{zk+\lambda}{2}} I_0(\sqrt{\lambda z}) dz.
 \end{aligned}
 \tag{47}$$

The following variable change $x = \sqrt{zk}$ gives:

$$\begin{aligned} \text{SER}(\gamma) &= 1 + \sum_{k=1}^{\epsilon+1} C_{N-1}^{k-1} \frac{(-1)^k}{k} \\ &\quad \times \int_{z_c}^{+\infty} e^{-\frac{x^2+\lambda}{2}} I_0\left(x\sqrt{\frac{\lambda}{k}}\right) x dx \\ &= 1 + \sum_{k=1}^{\epsilon+1} C_N^k \frac{(-1)^k}{N} \\ &\quad \times \int_{z_c}^{+\infty} e^{-\frac{x^2+\frac{\lambda}{k}-\frac{\lambda}{k}+\lambda}{2}} I_0\left(x\sqrt{\frac{\lambda}{k}}\right) x dx \\ &= 1 + \sum_{k=1}^{\epsilon+1} C_N^k \frac{(-1)^k}{N} e^{-\frac{(k+1)\lambda}{2k}} Q_1\left(\sqrt{\frac{\lambda}{k}}, \sqrt{kz_c}\right). \end{aligned} \quad (48)$$

And by replacing λ by his value we get the wanted result.

**APPENDIX B
PROOF OF THEOREM 1**

A. NAKAGAMI FADING

The Nakagami fading is defined with a single parameter m corresponding to the available diversity, which is a real value superior to 0.5. The pdf of the fading is given by [28]:

$$f_{|h|^2}(x) = \frac{m^m}{\Gamma(m)} x^{m-1} e^{-mx}, \quad (49)$$

where $\Gamma(x)$ is the gamma function. Reusing the expression of $f_{|h|^2}(x)$ in (37), we have to deal with the expression:

$$\begin{aligned} \text{SER}_{\text{Naka}}(\gamma) &= 1 + \frac{m^m}{\Gamma(m)} \sum_{k=1}^{\epsilon+1} C_N^k (-1)^k \\ &\quad \times \int_0^{\infty} e^{-\left(\frac{N\cdot\gamma(k-1)}{k} + m\right)x} Q_1\left(\sqrt{\frac{2N}{k}} x \gamma, \sqrt{kz_c}\right) x^{m-1} dx. \end{aligned} \quad (50)$$

This integral form including the Marcum function and an exponential was studied in previous works and [29] gives some solutions of the integral defined by:

$$\mathcal{F}(k, l, a, b, p) = \int_0^{\infty} e^{-px} Q_l(a\sqrt{x}, b) x^{k-1} dx. \quad (51)$$

Then, applying this result to our case, i.e., when k is the real Nakagami parameter and l is equal to 1, the solution is given by:

$$\begin{aligned} \mathcal{F}(m, 1, a, b, p) &= \frac{\Gamma(m)}{p^m} + \frac{2^m \Gamma(m) e^{-\frac{b^2}{2}}}{\tilde{p}} \\ &\quad \times \left({}_1F_1\left(m; 2; \frac{a^2 b^2}{2\tilde{p}}\right) - \Phi_2\left(1, m, 1; \frac{b^2}{2}, \frac{a^2 b^2}{2\tilde{p}}\right) \right). \end{aligned} \quad (52)$$

with the following parameters:

$$a = \sqrt{\frac{2N}{k}} \gamma, b = \sqrt{kz_c}, p = N\gamma \frac{k-1}{k} + m, \tilde{p} = a^2 + 2p. \quad (53)$$

Combining this result with (50),

$$\begin{aligned} \text{SER}_{\text{Naka}}(\gamma) &= 1 + m^m \sum_{k=1}^{\epsilon+1} \frac{C_N^k}{N} (-1)^k \frac{1}{p^m} + \frac{2^m e^{-\frac{b^2}{2}}}{\tilde{p}^m} \\ &\quad \times \left({}_1F_1\left(m; 2; \frac{a^2 b^2}{2\tilde{p}}\right) - \Phi_2\left(1, m, 1; \frac{b^2}{2}, \frac{a^2 b^2}{2\tilde{p}}\right) \right). \end{aligned} \quad (54)$$

The last step is to replace the parameters $a, b, p,$ and \tilde{p} , and simplify to obtain (38).

B. RICEAN FADING

The Ricean fading considers line of sight and multipaths of the main signal, and is defined by the parameter K representing the power ratio of those two parts [28]. The distribution of $|h/\sigma|^2$ follows a noncentral chi-squared law with 2 degrees of freedom, thus pdf of $|h|^2$ is expressed as follows:

$$f_{|h|^2}(x) = (1 + K)e^{-K} e^{-(1+K)x} I_0\left(2\sqrt{K(1+K)x}\right), \quad (55)$$

with $I_0(\cdot)$ the modified Bessel function of the second kind of order 0. The expression of the average SER over a Ricean fading is given by:

$$\begin{aligned} \text{SER}_{\text{Rice}}(\gamma) &= 1 + \frac{(1+K)e^{-K}}{N} \sum_{k=1}^{\epsilon+1} C_N^k (-1)^k \\ &\quad \times \int_0^{\infty} e^{-\left(\frac{2N\cdot\gamma(k-1)}{k} + K + 1\right)x} \\ &\quad \times Q_1\left(\sqrt{\frac{2N}{k}} x \gamma, \sqrt{kz_c}\right) I_0(2\sqrt{K(K+1)x}) dx. \end{aligned} \quad (56)$$

Previous interesting results can be found in [30] about integrals involving Marcum and Modified Bessel functions. The authors defined the function $\text{In}(\alpha, \beta, c, p, \mu_1, \mu_2)$ as [30, eq.(1)]:

$$\begin{aligned} \text{In}(a, b, c, p, \mu_1, \mu_2) &= \int_0^{+\infty} e^{-pt} Q_{\mu_1}(a\sqrt{t}, b) t^{\frac{\mu_2-1}{2}} I_{\mu_2-1}(c\sqrt{t}) dt. \end{aligned} \quad (57)$$

The expression of SER_{Rice} can be expressed as:

$$\begin{aligned} \text{SER}_{\text{Rice}}(\gamma) &= 1 + \frac{(1+K)e^{-K}}{N} \\ &\quad \times \sum_{k=1}^{\epsilon+1} C_N^k (-1)^k \text{In}(a, b, c, p, 1, 1), \end{aligned} \quad (58)$$

with the following parameters:

$$a = \sqrt{\frac{2N}{k}}\gamma, \quad b = \sqrt{kz_c}, \quad p = N\gamma \frac{k-1}{k} + (1 + \kappa), \quad (59)$$

$$c = 2\sqrt{\kappa(\kappa + 1)}. \quad (60)$$

The special case $\mu_1 = \mu_2 = 1$ leads to some simplifications and thanks to [30, eq.(22)]:

$$\begin{aligned} & \text{In}(a, b, c, p, 1, 1) \\ &= \frac{1}{p} e^{\frac{c^2}{4p}} Q_1 \left(\frac{ac}{\sqrt{2p(2p+a^2)}}, b\sqrt{\frac{2p}{2p+a^2}} \right). \end{aligned} \quad (61)$$

Replacing the expressions of $a, b, c,$ and p defined just above leads to the solution.

C. RAYLEIGH FADING

The Rayleigh fading is equivalent to a Nakagami special case with $m = 1$, therefore from (38) we get:

$$\begin{aligned} \text{SER}_{\text{Ray}}(\gamma) &= 1 + \frac{1}{N} \sum_{k=1}^{\epsilon+1} C_N^k (-1)^k \\ &\times \mathcal{F} \left(1, 1, \sqrt{\frac{2N}{k}}\gamma, \sqrt{kz_c}, \frac{(k-1)N}{k}\gamma + 1 \right), \end{aligned} \quad (62)$$

The expression of $\mathcal{F}(k, l, a, b, p)$ is available for $k = 1$ and $l = 1$ [29, eq.(22)]:

$$\mathcal{F}(1, 1, a, b, p) = \frac{e^{-\frac{pb^2}{a^2+2p}}}{p}. \quad (63)$$

The last step is to replace expressions of the parameters and the final equation is achieved.

APPENDIX C

PROOF OF THEOREM 2: HIGH-SNR SER APPROXIMATION

A. NAKAGAMI FADING

From (38), replacing $\bar{\gamma}/(\bar{\gamma} + 1)$ by 1 and reorganizing the sums leads to the wanted result.

B. RICEAN FADING

Considering the result (39) and applying $\bar{\gamma} \gg 1$, we obtain by separating the term where $k = 1$:

$$\begin{aligned} \text{SER}_{\text{Rice}}(\bar{\gamma}) &\simeq 1 - Q_1 \left(\sqrt{2K}, \sqrt{\frac{z_c}{\bar{\gamma}}} \right) \\ &+ \sum_{k=2}^{\epsilon+1} \frac{C_N^k}{N} (-1)^k \left(\frac{k-1}{\bar{\gamma}} \right)^{-1} \\ &\times e^{-K} Q_1 \left(0, \sqrt{z_c(k-1)} \right), \end{aligned} \quad (64)$$

As $Q_1(0, b) = e^{-\frac{b^2}{2}}$ and for small values of b :

$$Q_1(a, b) \simeq 1 - e^{-\frac{a^2}{2}} \left(1 - e^{-\frac{b^2}{2}} \right) \quad (65)$$

$$\simeq 1 - e^{-\frac{a^2}{2}} \frac{b^2}{2}, \quad (66)$$

the SER can be approximated by:

$$\begin{aligned} \text{SER}_{\text{Ray}}(\bar{\gamma}) &\simeq e^{-K} e^{-\frac{z_c}{2\bar{\gamma}}} \\ &+ \sum_{k=2}^{\epsilon+1} \frac{C_N^k}{N} (-1)^k \left(\frac{k-1}{\bar{\gamma}} \right)^{-1} e^{-K} e^{-\frac{z_c}{2}(k-1)}. \end{aligned} \quad (67)$$

C. RAYLEIGH FADING

The Rayleigh fading is just a special case of Ricean one with $K = 0$.

REFERENCES

- [1] G. A. Akpakwu, B. J. Silva, G. P. Hancke, and A. M. Abu-Mahfouz, "A survey on 5G networks for the Internet of Things: Communication technologies and challenges," *IEEE Access*, vol. 6, pp. 3619–3647, Dec. 2018.
- [2] M. Centenaro, L. Vangelista, A. Zanella, and M. Zorzi, "Long-range communications in unlicensed bands: The rising stars in the IoT and smart city scenarios," *IEEE Wireless Commun.*, vol. 23, no. 5, pp. 60–67, Oct. 2016.
- [3] F. A. Aoudia, M. Gautier, M. Magno, M. L. Gentil, O. Berder, and L. Benini, "Long-short range communication network leveraging LoRa and wake-up receiver," *Microprocessors Microsyst., Embedded Hardw. Des.*, vol. 56, pp. 184–192, Feb. 2018.
- [4] L. Davoli, L. Belli, A. Cilfone, and G. Ferrari, "From micro to macro IoT: Challenges and solutions in the integration of IEEE 802.15.4/802.11 and sub-GHz technologies," *IEEE Internet Things J.*, vol. 5, no. 2, pp. 784–793, Apr. 2018.
- [5] U. Raza, P. Kulkarni, and M. Sooriyabandara, "Low power wide area networks: An overview," *IEEE Commun. Surveys Tuts.*, vol. 19, no. 2, pp. 855–873, 2nd Quart., 2017.
- [6] R. Sanchez-Iborra and M.-D. Cano, "State of the art in LP-WAN solutions for industrial IoT services," *Sensors*, vol. 16, no. 5, p. 708, May 2016.
- [7] C. Goursaud and J. M. Gorce, "Dedicated networks for IoT: PHY / MAC state of the art and challenges," *EAI Endorsed Trans. Internet Things*, vol. 1, no. 1, Oct. 2015, Art. no. 150597.
- [8] A. Ikpehai, B. Adebisi, K. M. Rabie, K. Anoh, R. E. Ande, M. Hammoudeh, H. Gacanin, and U. M. Mbanaso, "Low-power wide area network technologies for Internet-of-Things: A comparative review," *IEEE Internet Things J.*, vol. 6, no. 2, pp. 2225–2240, Apr. 2019.
- [9] O. Seller and N. Sornin, "Low power long range transmitter," U.S. Patent 14 170 170, Aug. 7, 2014. [Online]. Available: <https://www.google.com/patents/US20140219329>
- [10] Semtech. (Mar. 2015). *SX1272/73–860 MHz to 1020 MHz Low Power Long Range Transceiver*. [Online]. Available: https://semtech.my.salesforce.com/sfc/p/#E0000000JelG/a/440000001NCE/v_VBhk1IolDgXwwnOpcS_vTFxPfSEPQbuneK3mWsXIU
- [11] A. Springer, W. Gugler, M. Huemer, L. Reindl, C. C. W. Ruppel, and R. Weigel, "Spread spectrum communications using chirp signals," in *Proc. IEEE/AFCEA EUROCOMM. Inf. Syst. Enhanced Public Saf. Secur.*, May 2000, pp. 166–170.
- [12] B. Reynders and S. Pollin, "Chirp spread spectrum as a modulation technique for long range communication," in *Proc. Symp. Commun. Veh. Technol. (SCVT)*, Nov. 2016, pp. 1–5.
- [13] D. Magrin, M. Centenaro, and L. Vangelista, "Performance evaluation of LoRa networks in a smart city scenario," in *Proc. IEEE Int. Conf. Commun. (ICC)*, Paris, France, May 2017, pp. 1–7.
- [14] F. Delobel, N. El Rachkidy, and A. Guitton, "Analysis of the delay of confirmed downlink frames in class b of LoRaWAN," in *Proc. IEEE 85th Veh. Technol. Conf. (VTC Spring)*, Sydney, NSW, Australia, Jun. 2017, pp. 1–6.
- [15] O. Georgiou and U. Raza, "Low power wide area network analysis: Can LoRa scale?" *IEEE Wireless Commun. Lett.*, vol. 6, no. 2, pp. 162–165, Apr. 2017.
- [16] H. H. R. Sherazi, M. A. Imran, G. Boggia, and L. A. Grieco, "Energy harvesting in LoRaWAN: A cost analysis for the industry 4.0," *IEEE Commun. Lett.*, vol. 22, no. 11, pp. 2358–2361, Nov. 2018.

- [17] Z. Ali, S. Henna, A. Akhuzada, M. Raza, and S. W. Kim, "Performance evaluation of LoRaWAN for green Internet of Things," *IEEE Access*, vol. 7, pp. 164102–164112, 2019.
- [18] L. Vangelista, "Frequency shift chirp modulation: The LoRa modulation," *IEEE Signal Process. Lett.*, vol. 24, no. 12, pp. 1818–1821, Dec. 2017.
- [19] J. G. Proakis and M. Salehi, *Digital Communications*, 5th ed. New York, NY, USA: McGraw-Hill, 1995.
- [20] C. Ferreira Dias, E. R. D. Lima, and G. Fraidenraich, "Bit error rate closed-form expressions for LoRa systems under Nakagami and rice fading channels," *Sensors*, vol. 19, no. 20, p. 4412, Oct. 2019, doi: 10.3390/s19204412.
- [21] T. Elshabrawy and J. Robert, "Closed-form approximation of LoRa modulation BER performance," *IEEE Commun. Lett.*, vol. 22, no. 9, pp. 1778–1781, Sep. 2018.
- [22] B. Reynders, W. Meert, and S. Pollin, "Range and coexistence analysis of long range unlicensed communication," in *Proc. 23rd Int. Conf. Telecommun. (ICT)*, May 2016, pp. 1–6.
- [23] G. Ferre and A. Giremus, "LoRa physical layer principle and performance analysis," in *Proc. 25th IEEE Int. Conf. Electron., Circuits Syst. (ICECS)*, Bordeaux, France, Dec. 2018, pp. 65–68.
- [24] J. Courjault, B. Vrigneau, M. Gautier, and O. Berder, "Accurate LoRa performance evaluation using marcum function," in *Proc. IEEE Global Commun. Conf. (GLOBECOM)*, Waikoloa, HI, USA, Dec. 2019, pp. 1–5.
- [25] J. Courjault, B. Vrigneau, and O. Berder, "Fast performance evaluation of LoRa communications over Rayleigh fading channels," in *Proc. Int. Workshop Math. Tools Technol. IoT mMTC Netw. Modeling, IEEE Wireless Commun. Netw. Conf. (WCNC)*, Marrakech, Morocco, Apr. 2019, pp. 1–5.
- [26] J. I. Marcum, *Table Q Functions*. Santa Monica, CA, USA: Rand Corporation, Jan. 1950.
- [27] E. Martos-Naya, J. M. Romero-Jerez, F. J. Lopez-Martinez, and J. F. Paris, "A MATLAB program for the computation of the confluent hypergeometric function ϕ_2 ," Repositorio Institucional Universidad de Málaga, Málaga, Spain, Tech. Rep., 2016. [Online]. Available: <https://riuma.uma.es/xmlui/handle/10630/12068>
- [28] M. D. Yacoub, "The κ - μ distribution and the η - μ distribution," *IEEE Antennas Propag. Mag.*, vol. 49, no. 1, pp. 68–81, Feb. 2007.
- [29] P. C. Sofotasios, S. Muhaidat, G. K. Karagiannidis, and B. S. Sharif, "Solutions to integrals involving the Marcum Q-function and applications," *IEEE Signal Process. Lett.*, vol. 22, no. 10, pp. 1752–1756, Oct. 2015.
- [30] N. Y. Ermolova and O. Tirkkonen, "Laplace transform of product of generalized Marcum Q, Bessel I, and power functions with applications," *IEEE Trans. Signal Process.*, vol. 62, no. 11, pp. 2938–2944, Jun. 2014.



OLIVIER BERDER (Member, IEEE) received the Ph.D. degree in electrical engineering from the University of Bretagne Occidentale, Brest, France, in 2002. After a postdoctoral position at Orange Labs, in 2005, he joined the Université de Rennes 1, France, where he is currently a Full Professor with IUT Lannion, and the Leader of the GRANIT Team of the IRISA Laboratory. He has coauthored more than 100 peer-reviewed papers in international journals and conferences and has

coordinated or participated in numerous collaborative projects funded by either European Union or French National Research Agency, mainly related to wireless sensor networks. His research interests include multi-antenna systems and cooperative techniques for energy efficient communications and wireless sensor networks.



MANAV R. BHATNAGAR (Senior Member, IEEE) received the M.Tech. degree in communications engineering from the Indian Institute of Technology Delhi, New Delhi, India, in 2005, and the Ph.D. degree in wireless communications from the Department of Informatics, University of Oslo, Oslo, Norway, in 2008.

From 2008 to 2009, he was a Postdoctoral Research Fellow with the University Graduate Center (UNIK), University of Oslo. He held visiting appointments with the Wireless Research Group, Indian Institute of Technology Delhi; the Signal Processing in Networking and Communications (SPINCOM) Group, University of Minnesota Twin Cities, Minneapolis, MN, USA; the Alcatel-Lucent Chair, SUPELEC, France; the Department of Electrical Computer Engineering, Indian Institute of Science, Bengaluru, India; the UNIK, University of Oslo; the Department of Communications and Networking, Aalto University, Espoo, Finland; and the INRIA/IRISA Laboratory, University of Rennes, Lannion, France. He is currently a Professor with the Department of Electrical Engineering, IIT Delhi, where he is also a Brigadier Bhopinder Singh Chair Professor. His research interests include signal processing for multiple-input-multiple-output systems, cooperative communications, non-coherent communication systems, distributed signal processing for cooperative networks, multiuser communications, ultrawideband-based communications, free-space optical communication, cognitive radio, software defined radio, power line communications, molecular communications, and satellite communications. He is also a Fellow of the Institution of Engineering and Technology (IET), U.K., the Indian National Academy of Engineering (INAE), the National Academy of Sciences, India (NASI), the Institution of Electronics and Telecommunication Engineers (IETE), India, and the Optical Society of India (OSI). He received the NASI-Scopus Young Scientist Award 2016 in engineering category, the Shri Om Prakash Bhasin Award in the field of Electronics & Information Technology for the year 2016, and the Hari Om Ashram Prerit Dr. Vikram Sarabhai Research Award 2017. He was selected as an Exemplary Reviewer of the IEEE COMMUNICATIONS LETTERS from 2010 to 2012, and the IEEE TRANSACTIONS ON COMMUNICATIONS in 2015. He is also an Editor of the IEEE TRANSACTIONS ON COMMUNICATIONS. He had been an Editor of the IEEE TRANSACTIONS ON WIRELESS COMMUNICATIONS from 2011 to 2014.



JULES COURJAULT received the M.Sc. degree in electronics from the Université de Rennes 1, France in 2019. From 2019 to 2020, he worked as a Research Engineer with the GRANIT Team of the IRISA Laboratory, where he is currently a Ph.D. Student. His research interests include the IoT, reinforcement learning, software defined radio, and energy efficient wireless communications.



BAPTISTE VRIGNEAU received the M.Sc. degree from the École Normale Supérieure of Cachan, France, in 2001, and the Ph.D. degree from the University of Brest, France, in 2006. From 2003 to 2007, he was a member of the Lab-STICC (formerly LEST), France. From 2008 to 2013, he was an Assistant Professor with the XLIM-SIC Laboratory, University of Poitiers, France. Since 2013, he has been an Assistant Professor with the Université de Rennes 1 and works the project team

GRANIT of the IRISA Laboratory, France. His research interests include MIMO systems, cooperation in wireless sensors networks and the IoT, and difficult environment and signal processing apply to smart grid (NILM).